Analysis of dike-induced stresses and deformation: new insights from Mt. Etna and SW Iceland

Noemi Corti[1], Alessandro Tibaldi[1,2], Fabio L. Bonali[1,2]

1. Department of Earth and Environmental Sciences, University of Milan-Bicocca, 20126 Milan, Italy;
2. CRUST-Interuniversity Center for 3D Seismotectonics with Territorial Applications, 66100 Chieti Scalo, Italy

Introduction

- During volcanic eruptions, magma is transported up to the surface through magma-filled fractures, referred to as **vertical dikes** or **inclined sheets**

- In most cases dikes **arrest in the crust**, not leading to an eruption

- In shallow settings, dike propagation can lead to **deformation at the topographic surface**, with the formation of fissures and normal faults

- Sometimes, dikes arrest at very shallow depths without causing brittle deformation. Understanding why this occurs is important for volcanic hazard assessment.

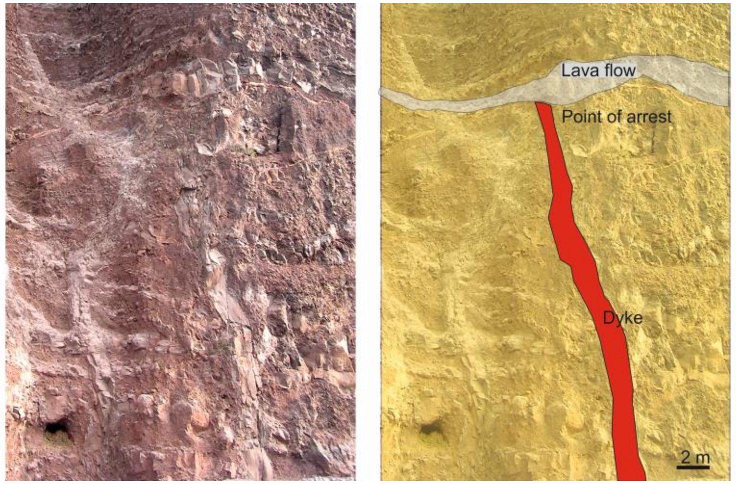

Example of arrested dike (Tibaldi, JVGR, 2015)

Dike-induced graben in the Krafla Fissure Swarm, Iceland (Tibaldi et al., JVGR, 2020)

Introduction

- **Analytical, analogue and numerical models** have been used to study the relation between surface deformation and dike intrusion (e.g., Pollard et al., 1983; Okada, 1985; Trippanera et al., 2015), crucial for volcanic hazard assessment and monitoring during an eruption

For example, Pollard et al. (1983) proposed the "dike rule", suggesting that the width of the dike-induced graben should be about twice the depth of the dike tip

<u>BUT…</u> more field observations are needed to anchor these models to realistic field cases

In nature, relations between dike geometry and surface deformation are **more complicated**, because the crust is **not homogeneous**

Numerical modeling integrated with **field data** can be used to overcome this limitation

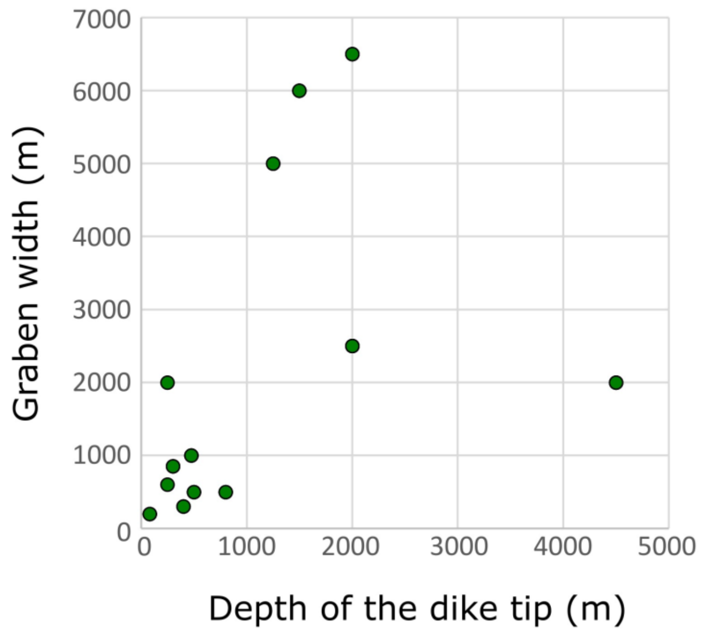

Data from literature review (Corti, 2024)

Goals and case studies

Methodologies:

- Collection of **new geological-structural and stratigraphic data**, thanks to classical fieldwork and 2D and 3D models reconstructed through Unmanned Aerial Vehicles (UAVs) and historical aerial photographs;
- Integration with **numerical modeling**, using the Finite Element Method (FEM) software COMSOL Multiphysics®

Case studies:

- 1928 eruptive fissure (Mt. Etna)
- 1971 eruptive fissure (Mt. Etna)
- Younger Stampar eruptive fissure (SW Iceland)

} Graben formation

Objectives

- Analyzing which parameters favor or inhibit **dike-induced surface deformation**
- Investigating what affects the **geometry of dike-induced graben faults**
- Understanding which parameters can favor the **arrest or the propagation** of a dike

Methodologies – structural data collection

Fieldwork survey

- **Classification** of all the structures visible in the field
- Collection of **quantitative structural data**

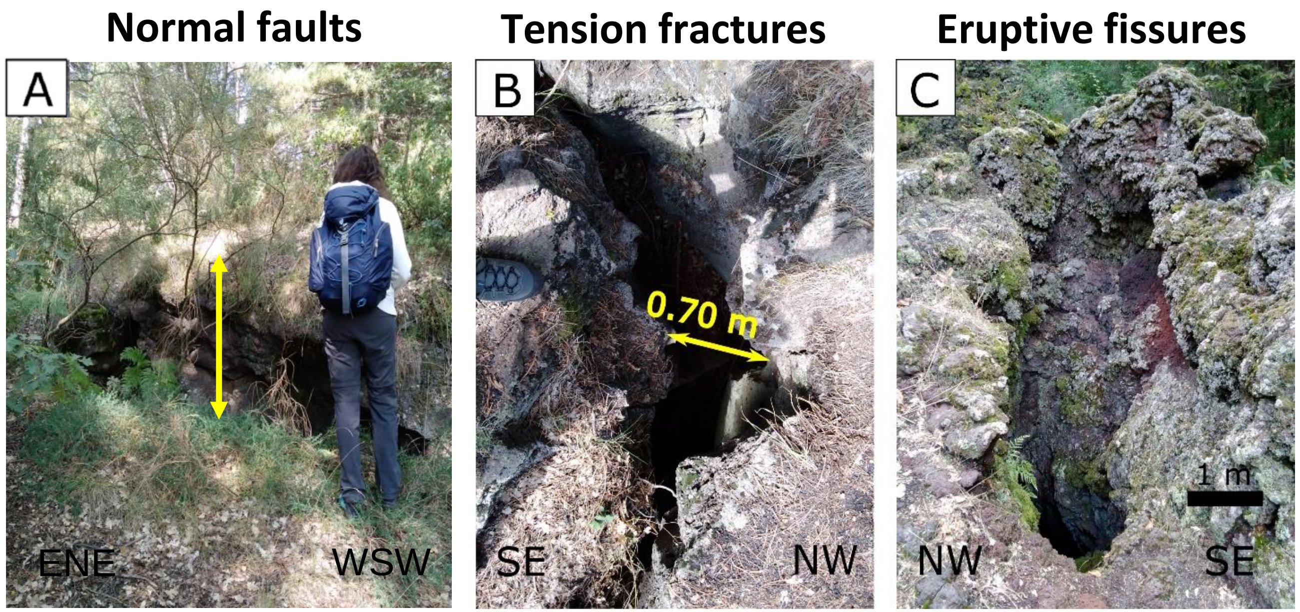

Examples of structures seen in the field on Mt. Etna

Analysis on 2D and 3D models reconstructed through Structure-from-Motion (SfM) photogrammetry

- **Historical aerial** photographs
- **UAV-collected** photographs

↓

Software for SfM (Agisoft Metashape)

↙ ↘

- Orthomosaics
- Digital Surface Models (DSMs)

3D models

↓

Immersive Virtual Reality

Methodologies – numerical modeling

Numerical modeling using the Finite Element Method software **COMSOL Multiphysics**, based on the collected structural data.

- **Basaltic dike** modeled as a **cavity** with an internal **overpressure** (P_0) in an elastic layered medium:

  Poisson's ratio (ν) = 0.25

  Density (ρ) and **Young's modulus (E)** based on typical values from the literature (Gudmundsson et al., 2011, 2020; Drymoni et al., 2020)

- All models fastened at the bottom edge to avoid rigid-body rotation and translation.

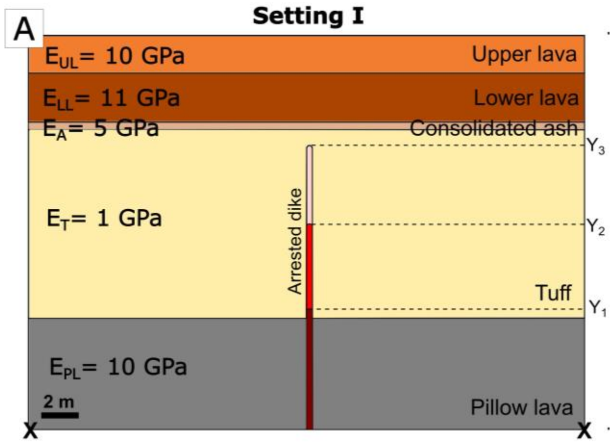

- To assess the probability of fracturing and of dike arrest/propagation, **tensile stress** (σ_3), absolute **shear stress** (τ) and **von Mises stress values** (τ) were plotted, and **σ_1 and σ_3 orientations** were also plotted as arrow surfaces.

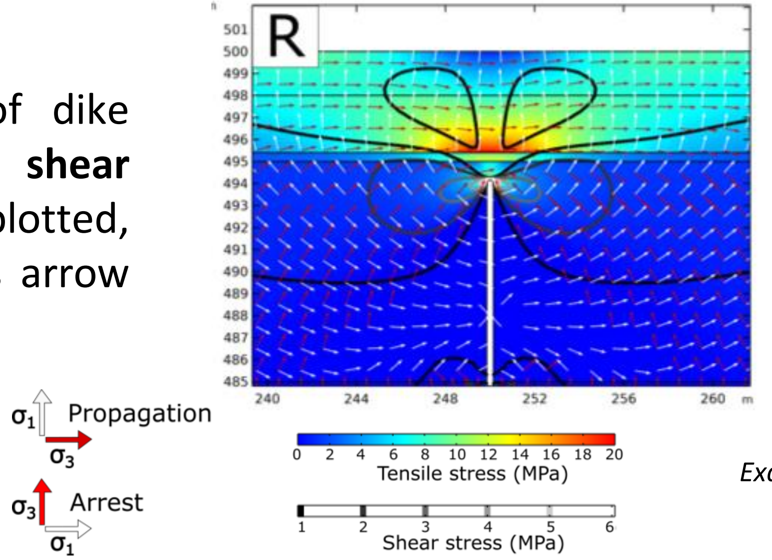

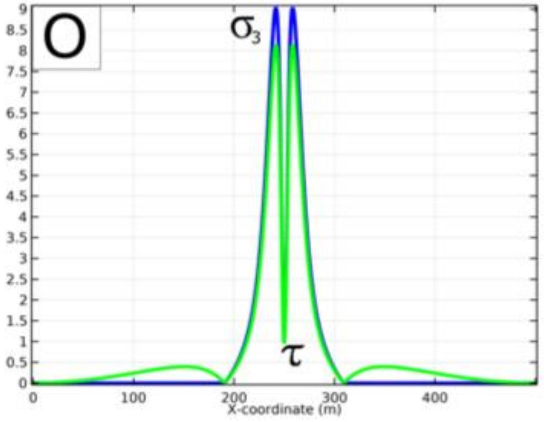

Examples of numerical models; setup and results (Corti et al., JVGR, 2023)

Mt. Etna – Geological setting

- Located in a compressional environment at the border between the African and the European Plate
- Several km-long faults of tectonic and volcanotectonic origin
- Slow gravitational spreading towards east affecting the eastern flank

For my project, I focused on an area located to the NE of the northern escarpment of the Valle del Bove, the **ENE rift**

1928 Fissure　　**1971 Fissure**

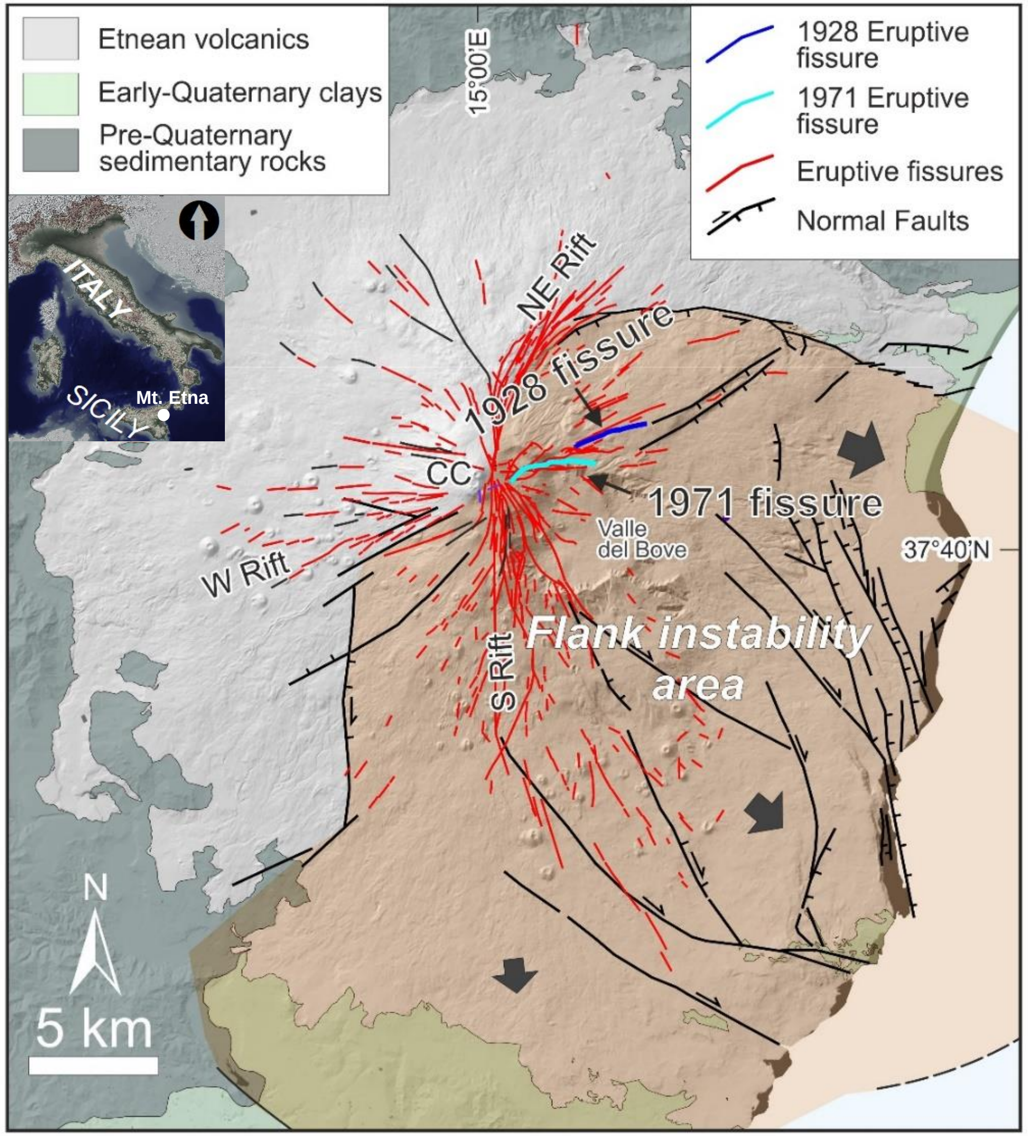

Modified after Bonali et al. (submitted)

Case study 1 – 1928 fissure (Mt. Etna)

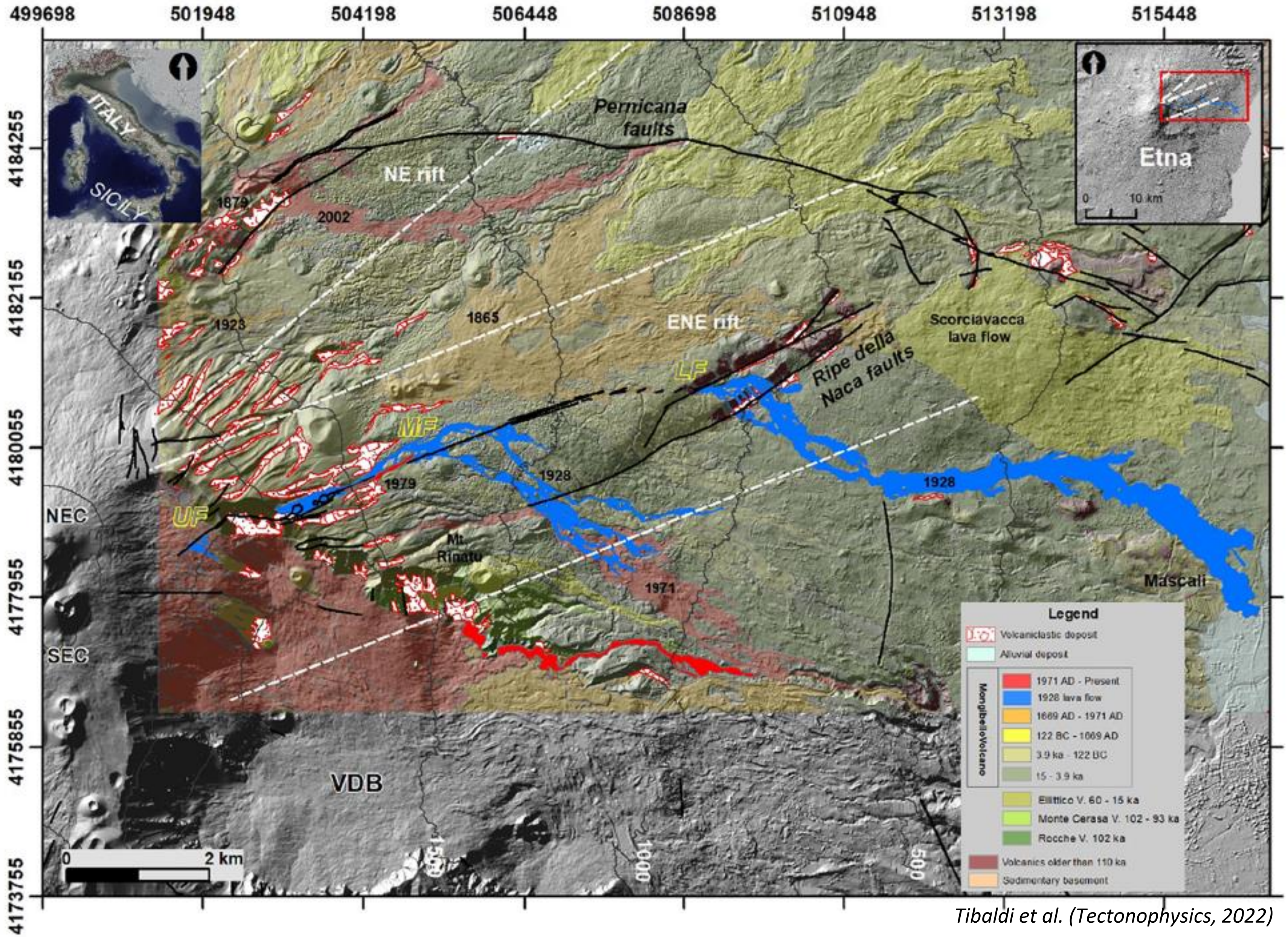

Tibaldi et al. (Tectonophysics, 2022)

Goals:

- Reconstructing the geometry of a system of **faults** and **fissures** associated with the **1928 volcanic activity** along the NE flank of **Mt. Etna**.
- Contributing to a better understanding of magma path and dike-induced surface deformation in active volcanic areas.

Case study 1 – Structural data

Four different settings of surface deformation were identified:

1) a sequence of eruptive vents, with the presence of a wide graben

2) a single eruptive fissure, without the formation of a graben

3) Half-graben and symmetric graben without eruption

4) Alignment of vents along the pre-existing Ripe della Naca faults

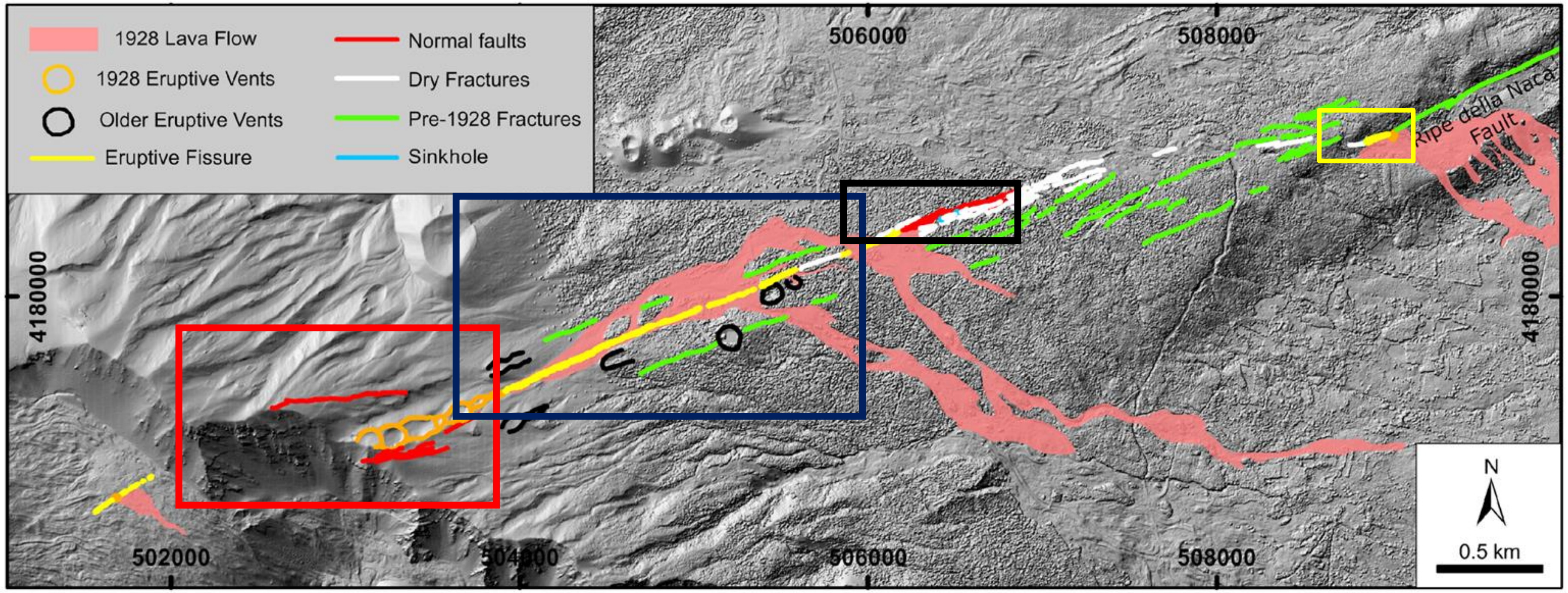

modified after Tibaldi et al. (Tectonophysics, 2022)

- What are the factors that affect **surface deformation**?
- Why are there differences within the 1928 fissure, which was induced by the same dike?

Case study 1 – Numerical modeling

Numerical models were run to investigate the parameters that affect the **distribution** and **concentration of stresses above the tip of the dike**

Model setup

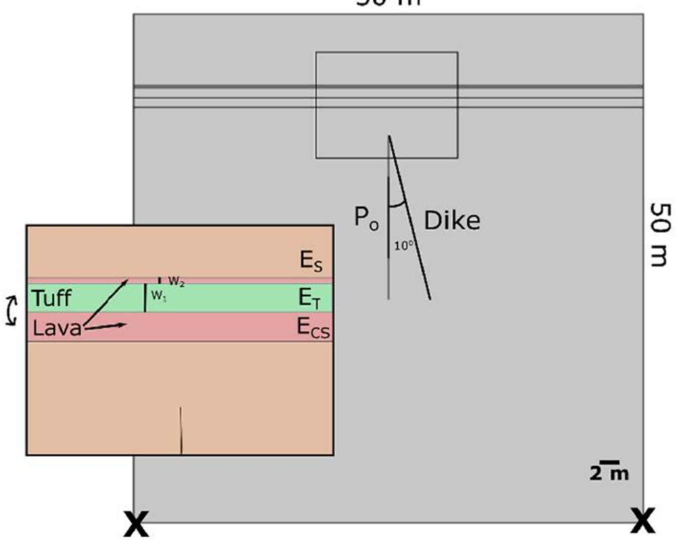

First, models were run using the **stratigraphy observed in the field,** changing only the **dike overpressure**

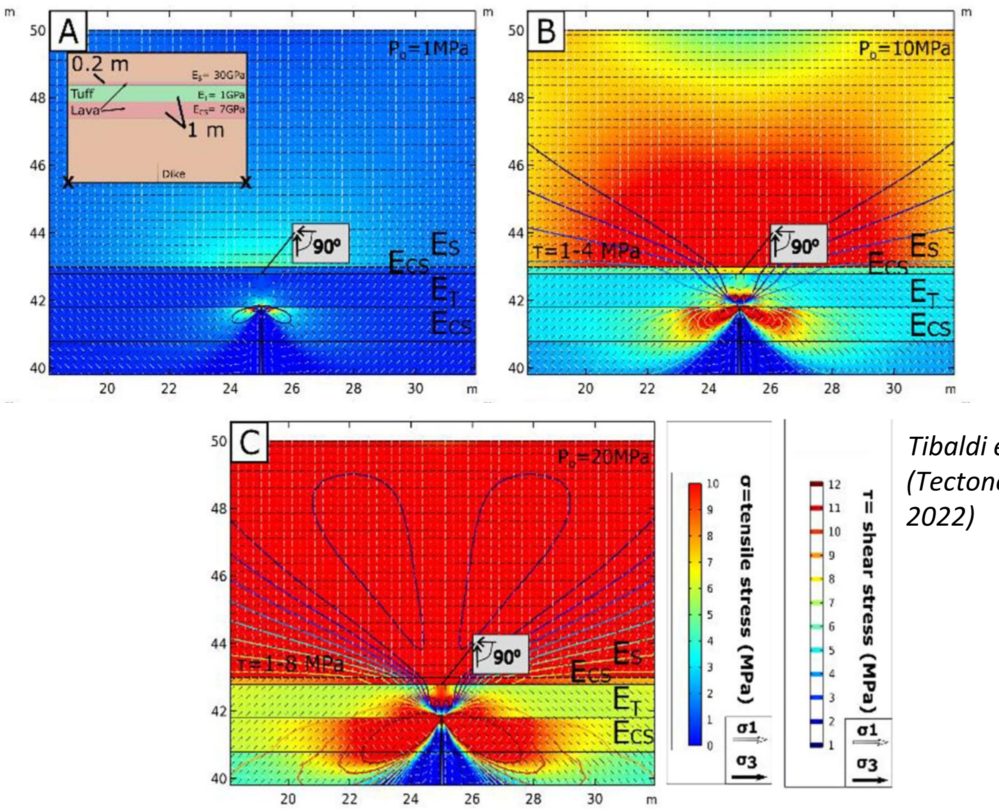

Tibaldi et al. (Tectonophysics, 2022)

- Tensile stress concentrates more in stiffer lavas;
- At the contact between tuff and lava, stresses rotate of 90°;
- With higher overpressure, shear stress contours are closer to the surface and tensile concentration is higher.

Case study 1 – Numerical modeling

Model setup

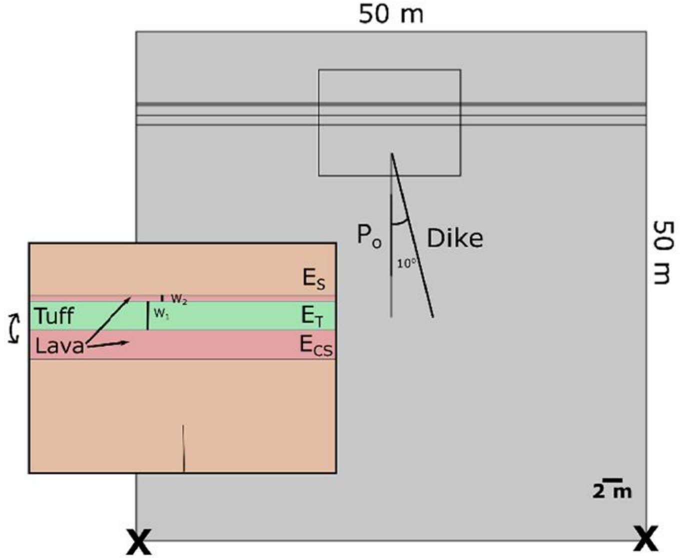

Then, **sensitivity analyses** were conducted, changing the **stratigraphy** of the host rock and the **inclination** of the dike.

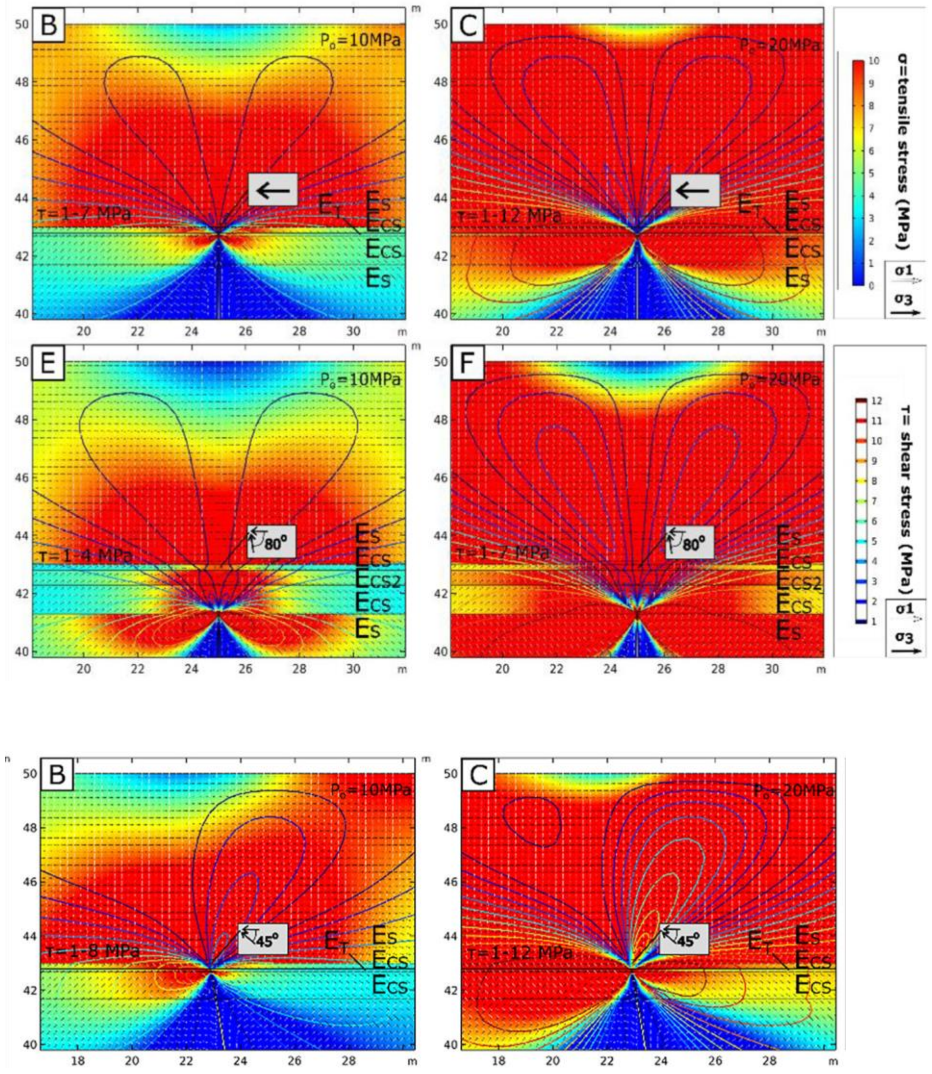

Tibaldi et al. (Tectonophysics, 2022)

Thinner tuff layer:

- Shear stress distributes closer to the surface with greater magnitudes;
- No stress rotation.

No tuff layer:

- Shear stress distributes closer to the surface, with more distant lobes.

Inclined dike:

- Concentration of stresses is asymmetrical.

Case study 2 – 1971 Fissure (Mt. Etna)

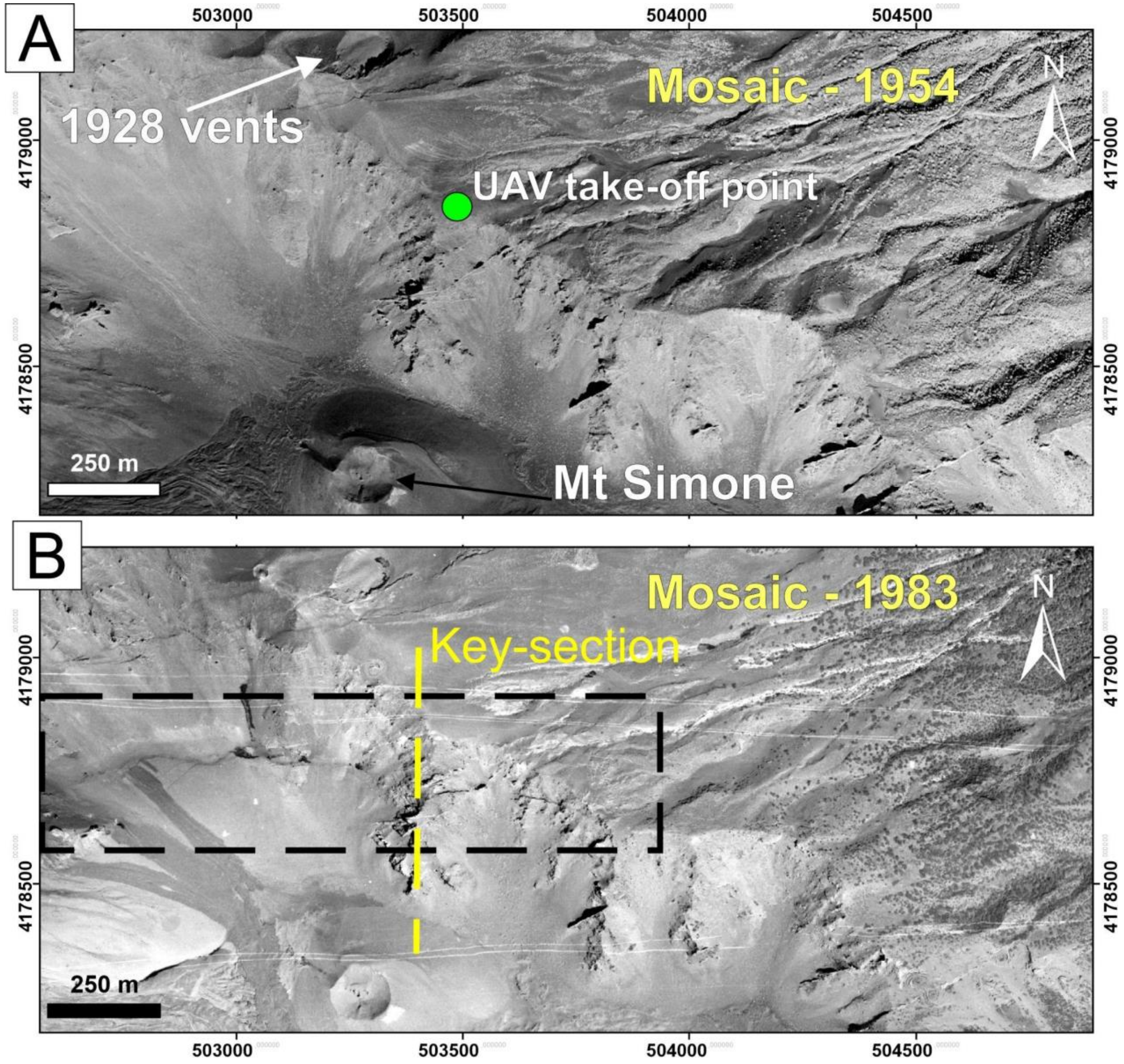

Bonali et al. (submitted)

Goals

- Quantifying the deformation associated with the **1971 dike intrusion**, with special attention to a **dike-induced graben** fully exposed in **section view**;
- Understanding which factors caused the **asymmetry** in the geometry of the dike-induced graben.

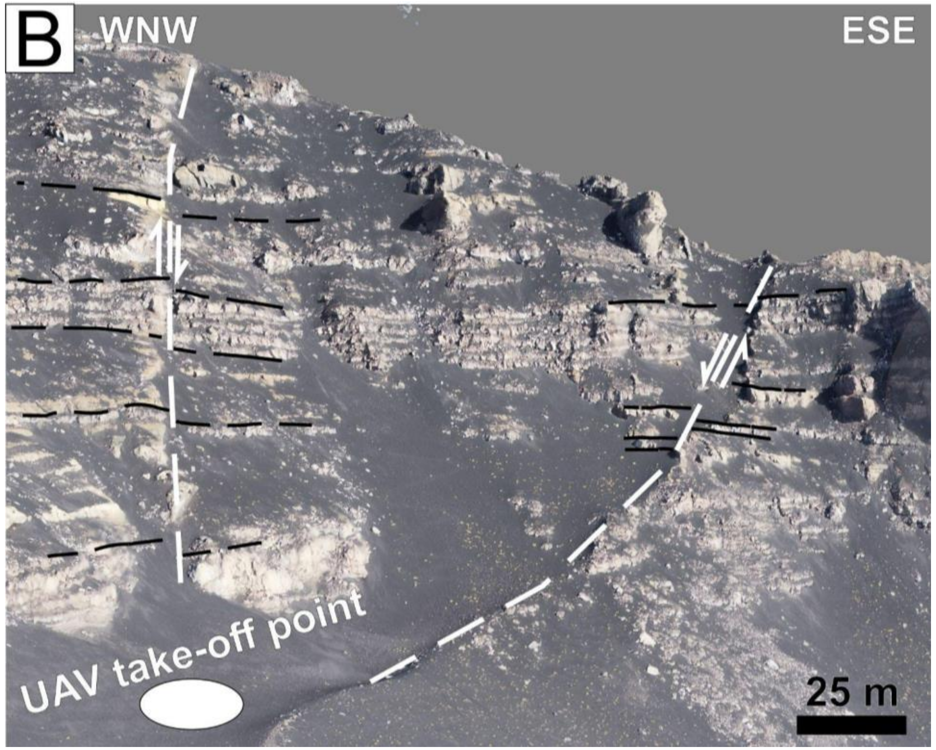

Drone-SfM derived 3D model (resolution of 5.5 cm/pix), from Bonali et al. (submitted)

Case study 2 – Structural data

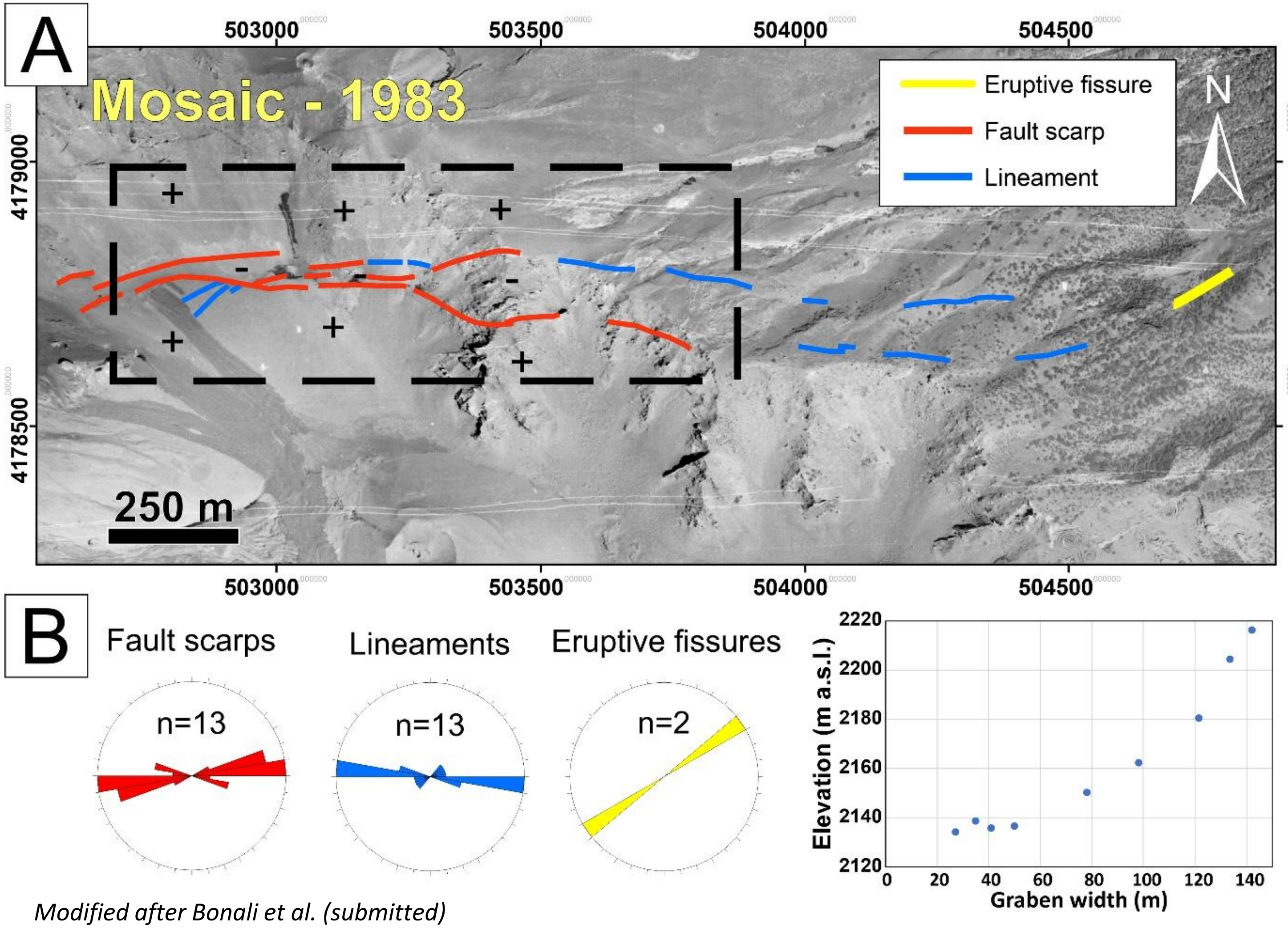

Modified after Bonali et al. (submitted)

<u>Structural data</u>

- **Graben structure**: 2 km-long, overall E-W trend;
- **Graben width** increases with an increase of the elevation;
- In section view, **faults dip angle** is 70° for the south-dipping fault, and 50° for the north-dipping one;

Case study 2 – Numerical modeling

Numerical models were run using to investigate the parameters that affect the **distribution** and **orientation of stresses**

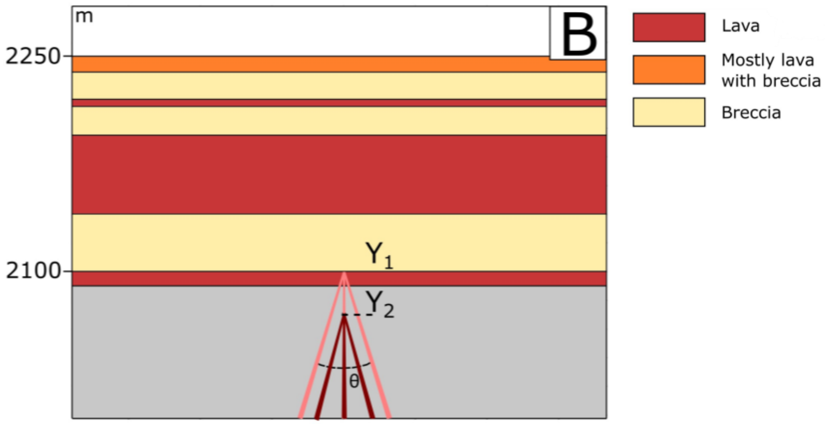

First, models were run using the **stratigraphy observed in the field,** with an overpressure of 6 MPa, changing the **dike inclination**

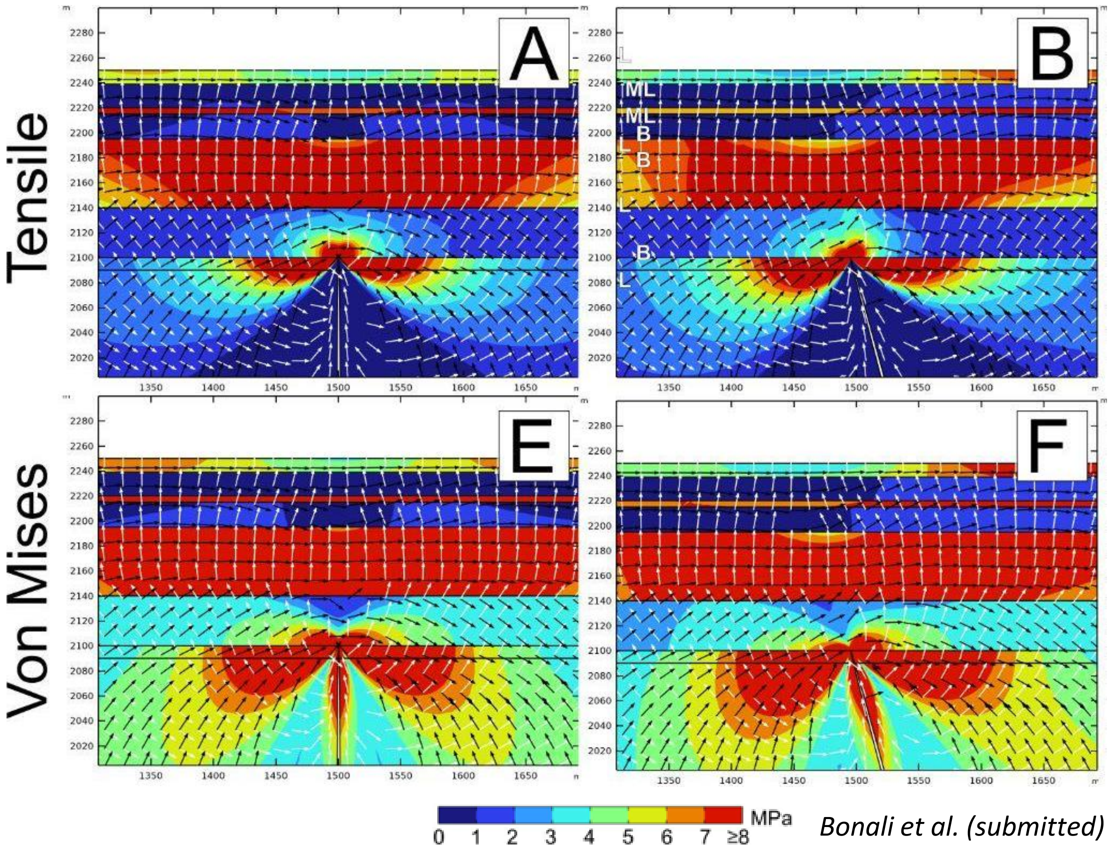

Bonali et al. (submitted)

- When the **host rock is layered**, soft layers suppress both tensile and von Mises stresses, that concentrate in the stiffer lava layers;
- The **inclination of the dike** causes an asymmetrical distribution of stresses and a clockwise rotation of σ_1 and σ_3;

Case study 2 – Numerical modeling

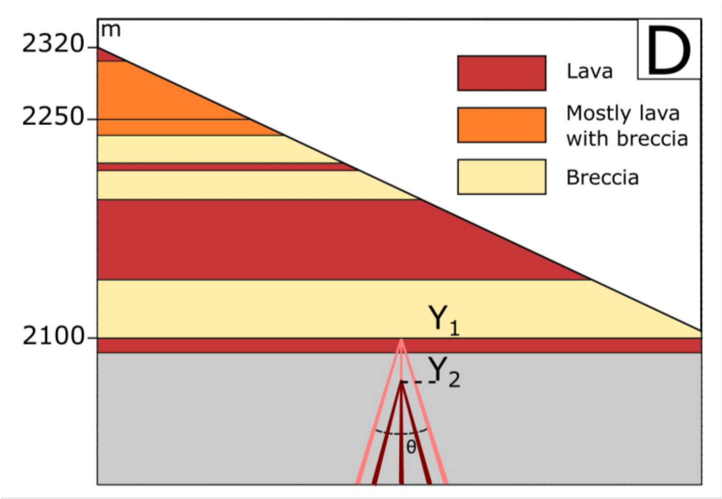

Then, the upper boundary has been designed with a 25° inclination, to better reproduce the **topography** of the study area

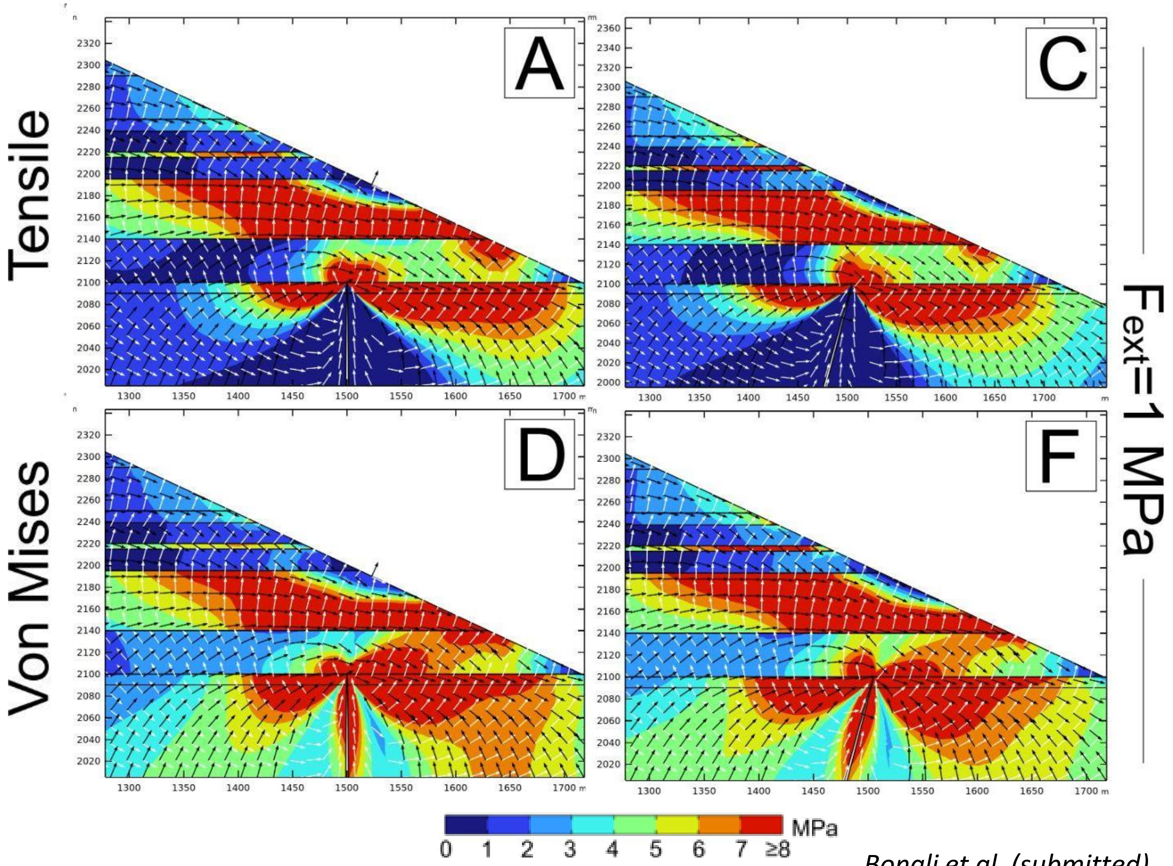

Bonali et al. (submitted)

- **Topography plays a key role** in determining the asymmetry of the faults, causing an asymmetrical distribution of stresses and a clockwise rotation of σ_1 and σ_3, even with a vertical dike.

SW Iceland – Geological setting

Reykjanes Peninsula (SW Iceland)

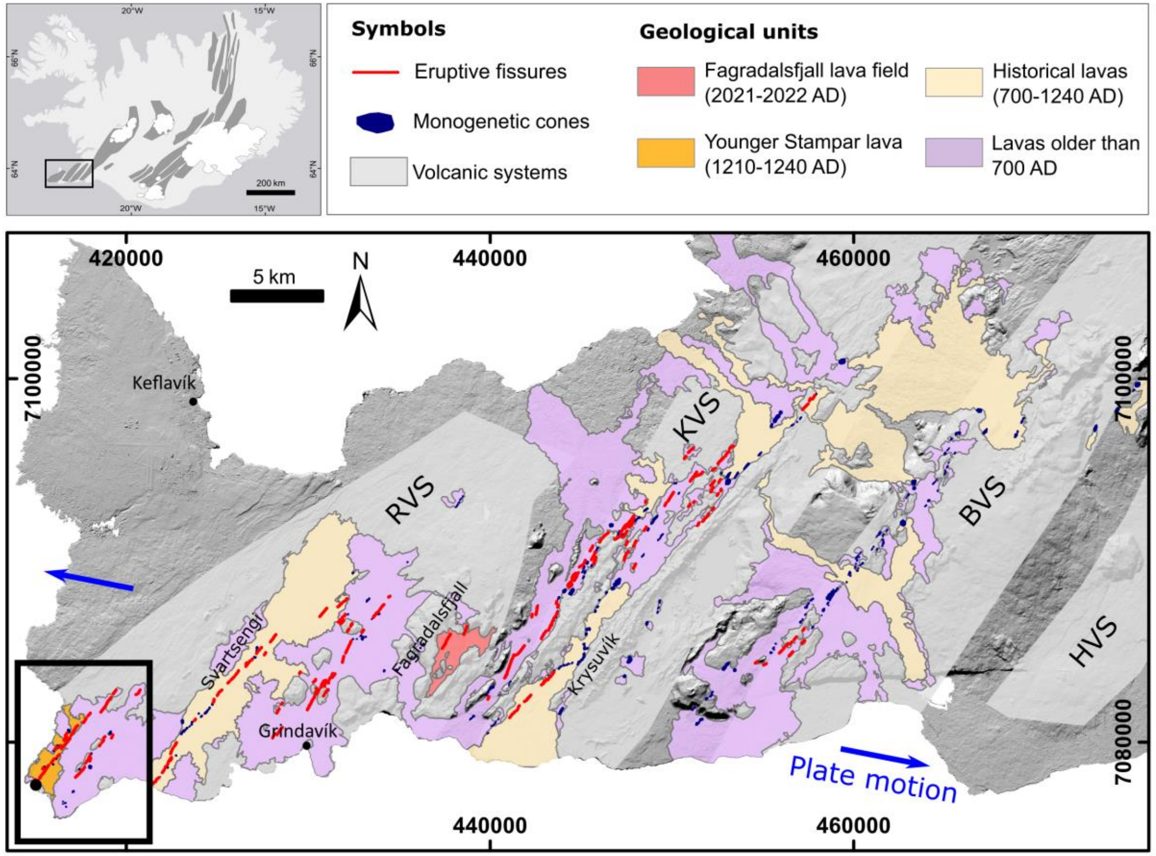

Before the volcanic activity in 2021-2023 at Fagradalsfjall, the latest volcanic episode took place between 700 and 1240 AD (Saemundsson et al., 2016, 2020)

Younger Stampar eruption, 1210-1240 AD (Saemundsson et al., 2016)

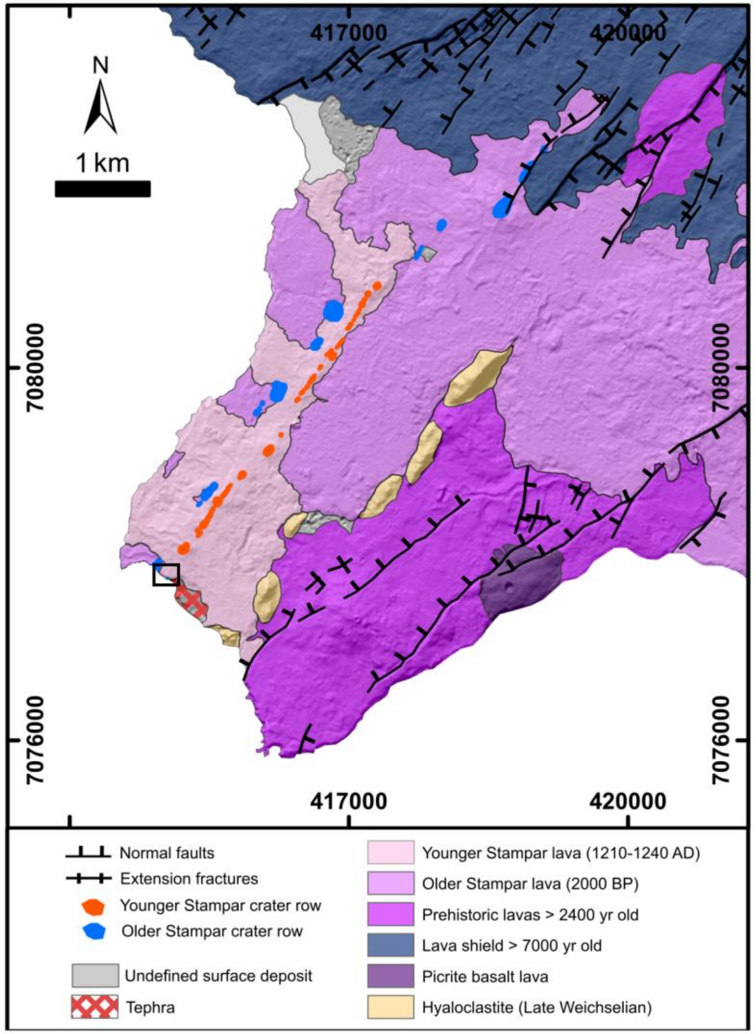

Corti et al. (JVGR, 2023)

Case study 3 – Younger Stampar fissure

Goals

- Understanding what caused the **arrest** of one dike, located only at 30 m from a **feeder dike**;
- Understanding **the absence of faults or tension fractures** at the surface, even if the dike arrested at a very shallow depth (5 m below the surface).

Feeder dike **Arrested dike**

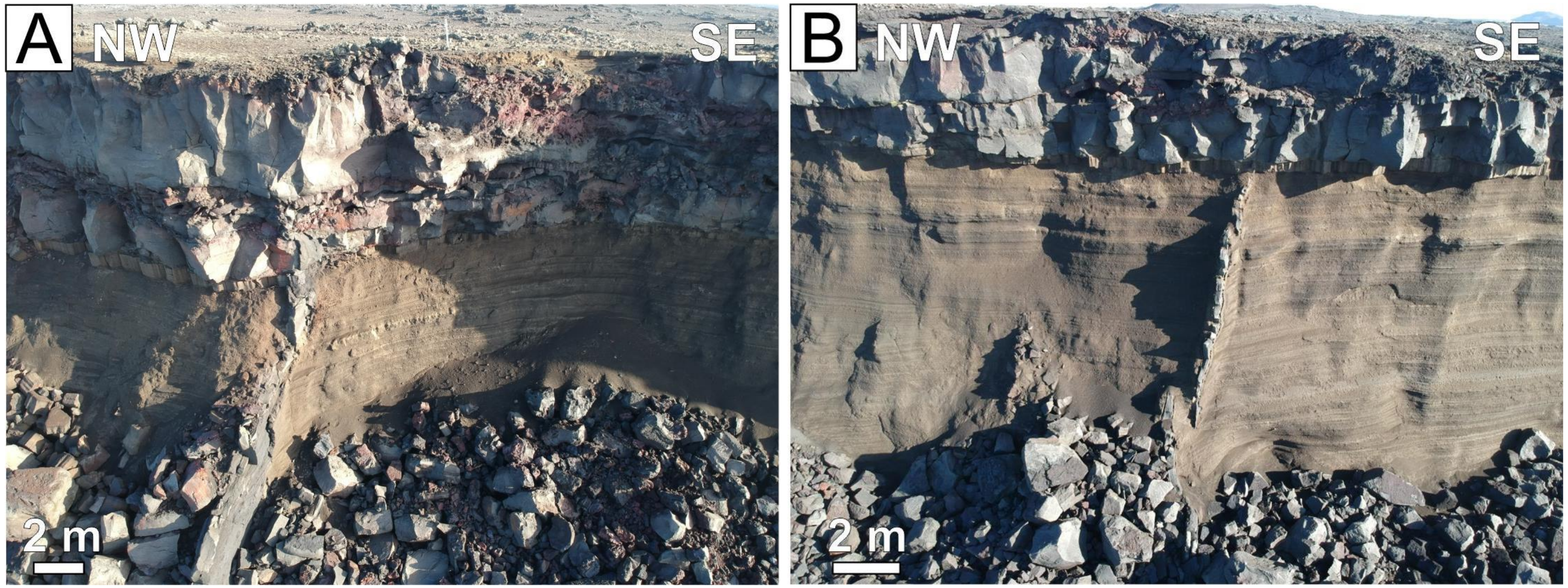

Drone-collected images of the studied dikes (Corti et al., JVGR, 2023)

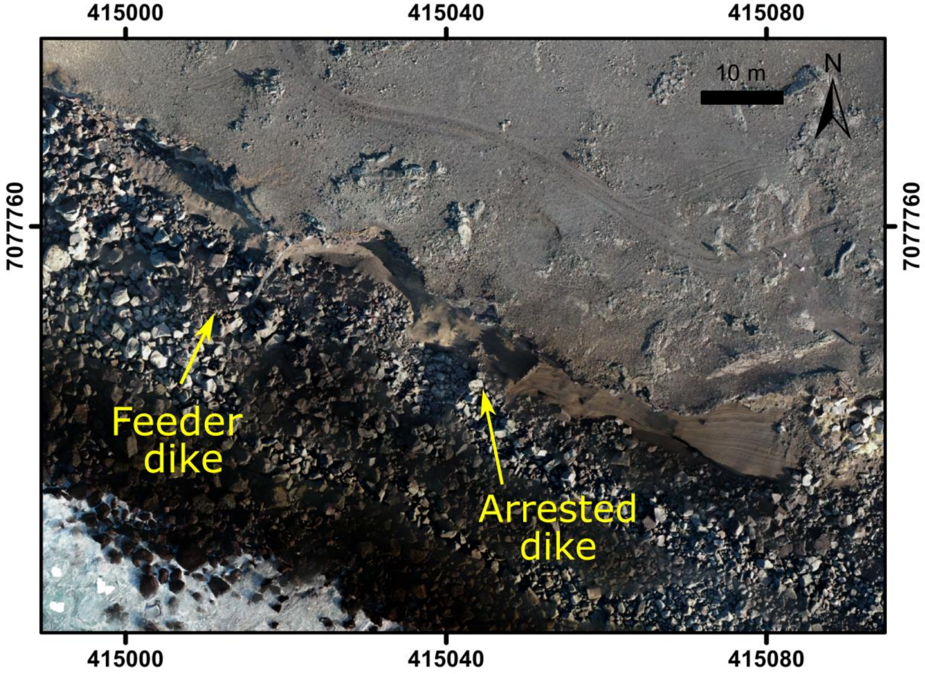

Drone-SfM derived orthomosaic of the studied outcrop (Corti et al., JVGR, 2023)

Case study 3 – Structural data

Studied outcrop and dikes

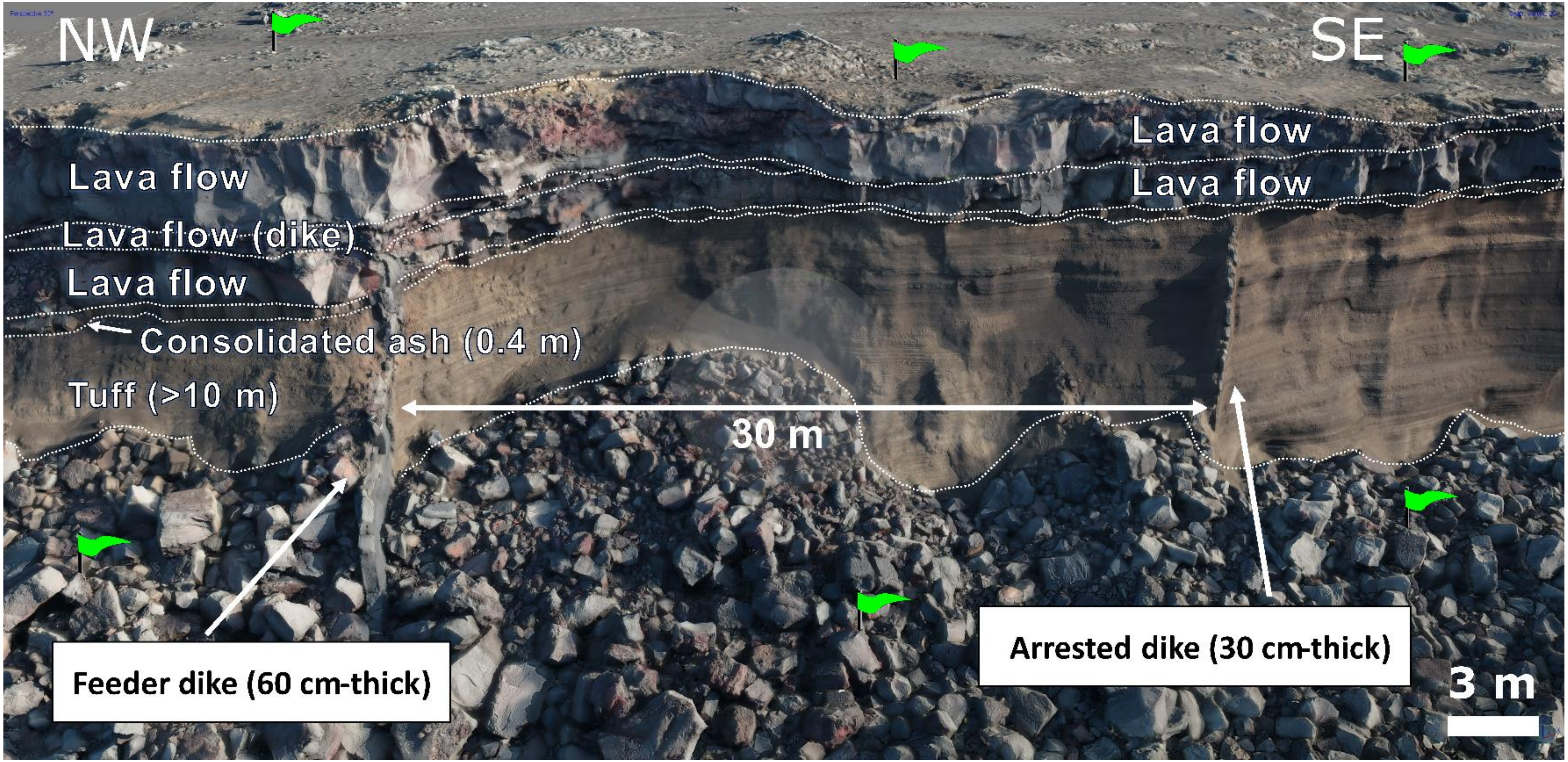

3D model derived from 1120 drone-collected pictures, Model resolution: 8 mm/pixel

Corti et al. (JVGR, 2023)

Case study 3 – Numerical modeling

Numerical models: setup

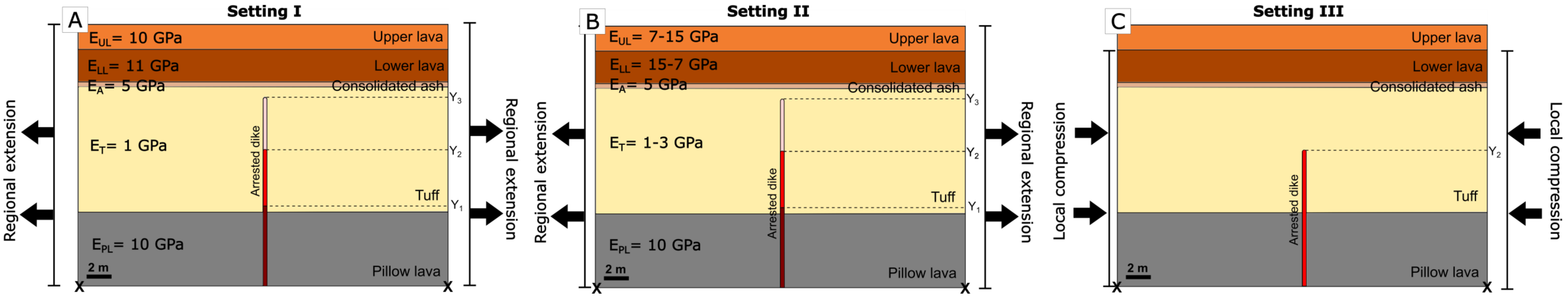

Corti et al. (JVGR, 2023)

Investigating **dike propagation in the tuff** layer

- three **dike tip locations** within the tuff
- different $\mathbf{P_0}$ (2-4 MPa)
- **extensional stress field** of 1 MPa

Exploring **layer properties** and how they affect dike propagation

- range of tuff's Young modulus (E) of 1-3 GPa
- range of lava layers' E of 7-15 GPa

Evaluating the influence of **compression caused by the previous intrusion of the feeder dike**.

- different P_0 (2-4 MPa)
- compressional stress field (2-4 MPa)

Case study 3 – Numerical modeling

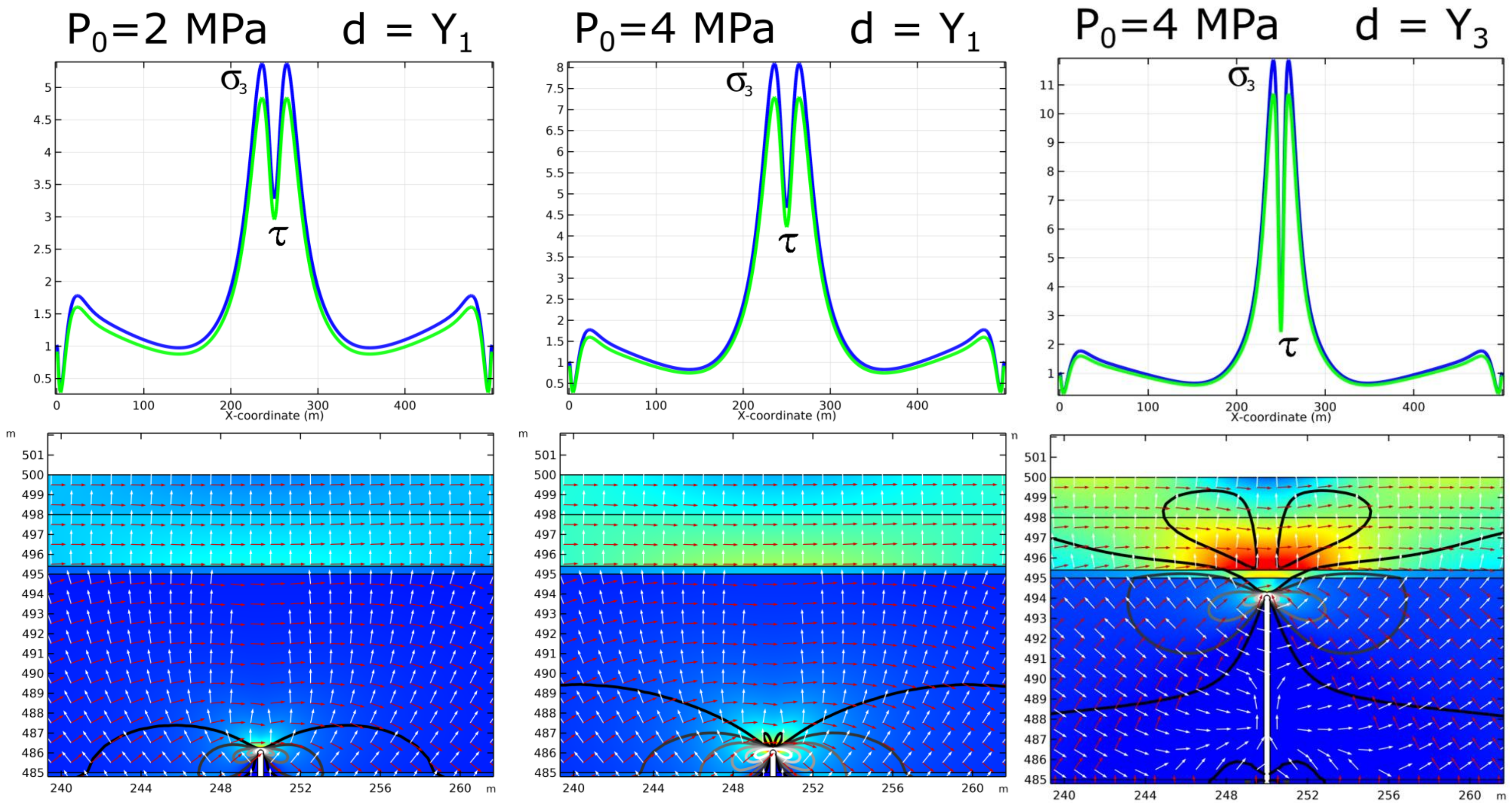

Corti et al. (JVGR, 2023)

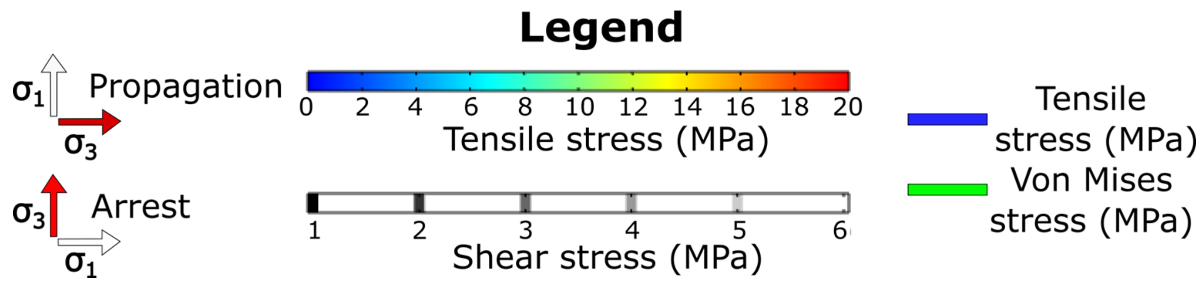

All the models are subject to an extensional stress field of 1 MPa

- Regardless of the dike overpressure, **no stress rotation** occurs at the dike tip;
- Increasing the **overpressure**, the magnitude of stresses at the tip of the dike and at the surface increases;
- While the dike moves closer to the **tuff-lava contact,** the concentration of **tensile stress decreases at the dike tip** and **increases in the stiffer lava layers**.

Case study 3 – Numerical modeling

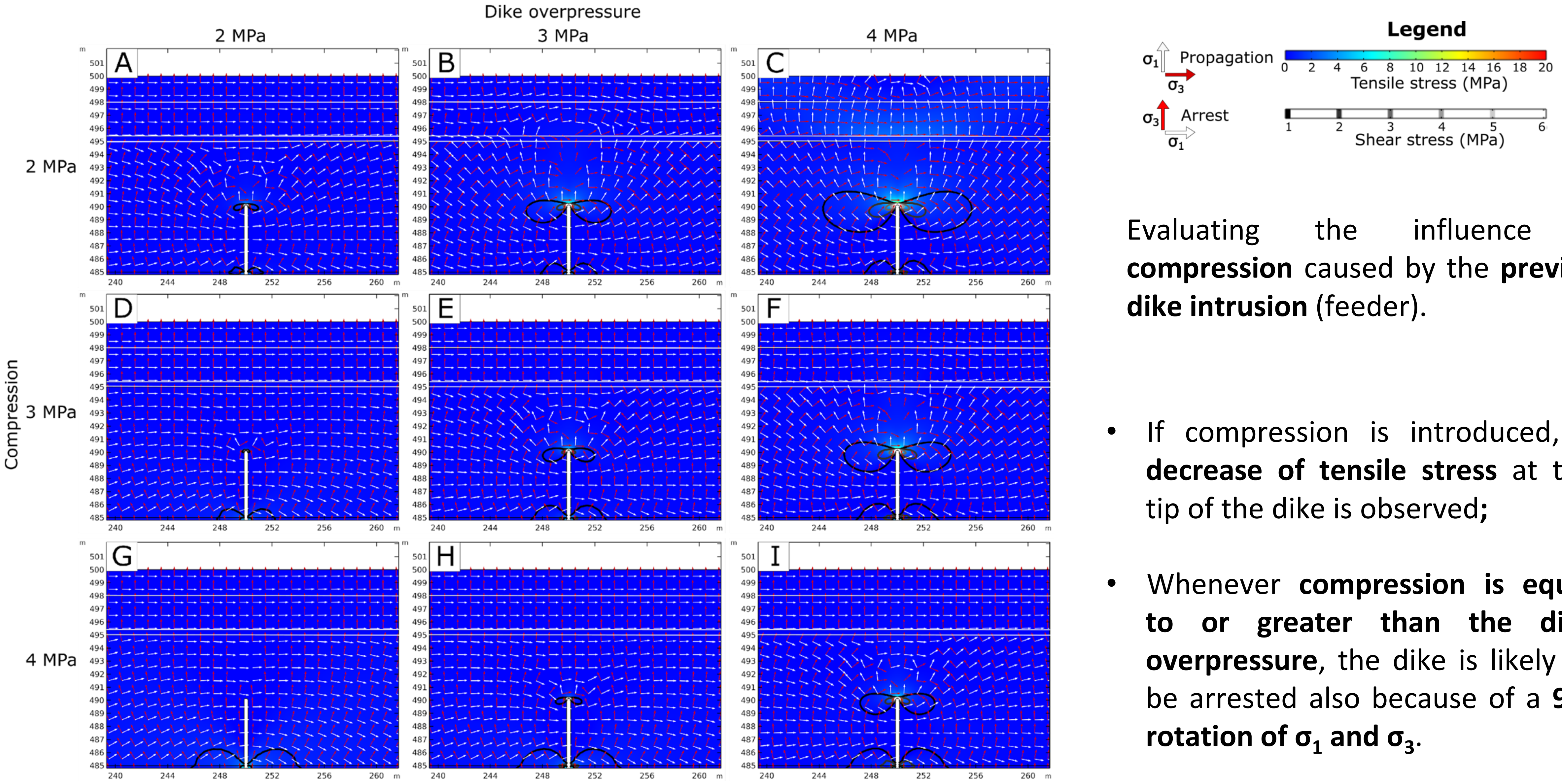

Corti et al. (JVGR, 2023)

Evaluating the influence of **compression** caused by the **previous dike intrusion** (feeder).

- If compression is introduced, a **decrease of tensile stress** at the tip of the dike is observed**;**
- Whenever **compression is equal to or greater than the dike overpressure**, the dike is likely to be arrested also because of a **90° rotation of σ_1 and σ_3**.

Discussion

Three main topics are analyzed: which **parameters favor (or inhibits) dike-induced deformation at the surface**, what affects **the geometry of dike-induced graben faults,** and which **parameters can favor the arrest of the dike?**

Which parameters favor or inhibit dike-induced surface deformation?

- **Overpressure**: a decrease results in a **decrease of tensile stress above the dike tip**. To have fracturing, tensile stress should be at least equal to the tensile strength of the crustal rocks (2-4 MPa, Gudmundsson, 2011).
- **Layering: stiff materials concentrate tensile stress**, favoring fracturing; **soft layers suppress stress** above the dike tip.
- **Extensional/compressional stress field**: **extension increases stresses** in stiff layers, whereas **compression reduces stresses at the tip**. Compression could be explained by previous intrusions of feeder dikes, as in the Stampar case study.

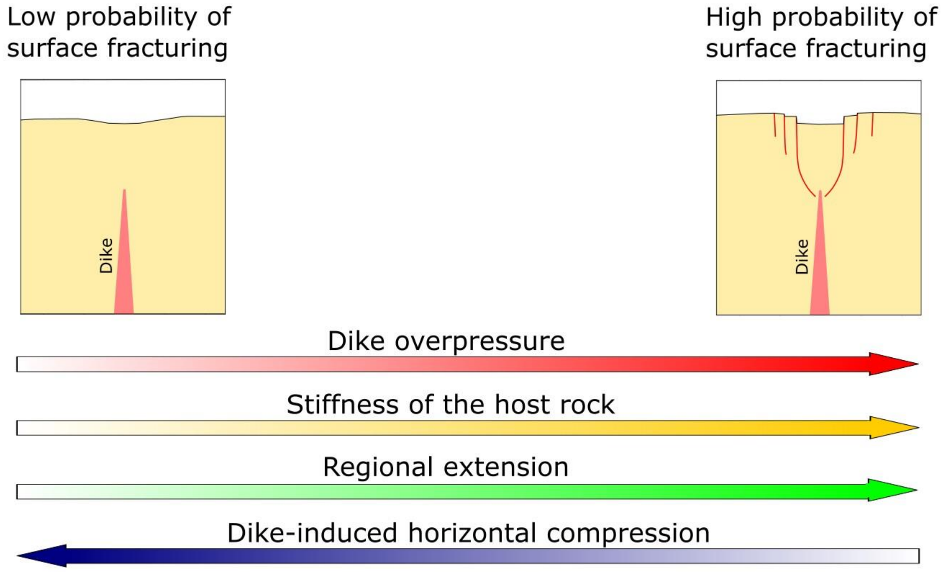

Corti (2024)

Discussion

What affects the geometry of dike-induced graben faults?

First, we summarized the geometrical features of 29 dike-induced grabens reported in the literature, both along **slow, intermediate, and fast spreading plate boundaries, and on volcanic edifices**. **New data** from Mt. Etna 1928 and 1971 grabens were also added.

- Grabens formed on **volcanic edifices** have the smallest offset and relatively small width.
- Grabens formed along **slow spreading ridges** are the widest and the longest.
- Grabens formed along **fast and intermediate spreading ridges** are the narrowest and the deepest.

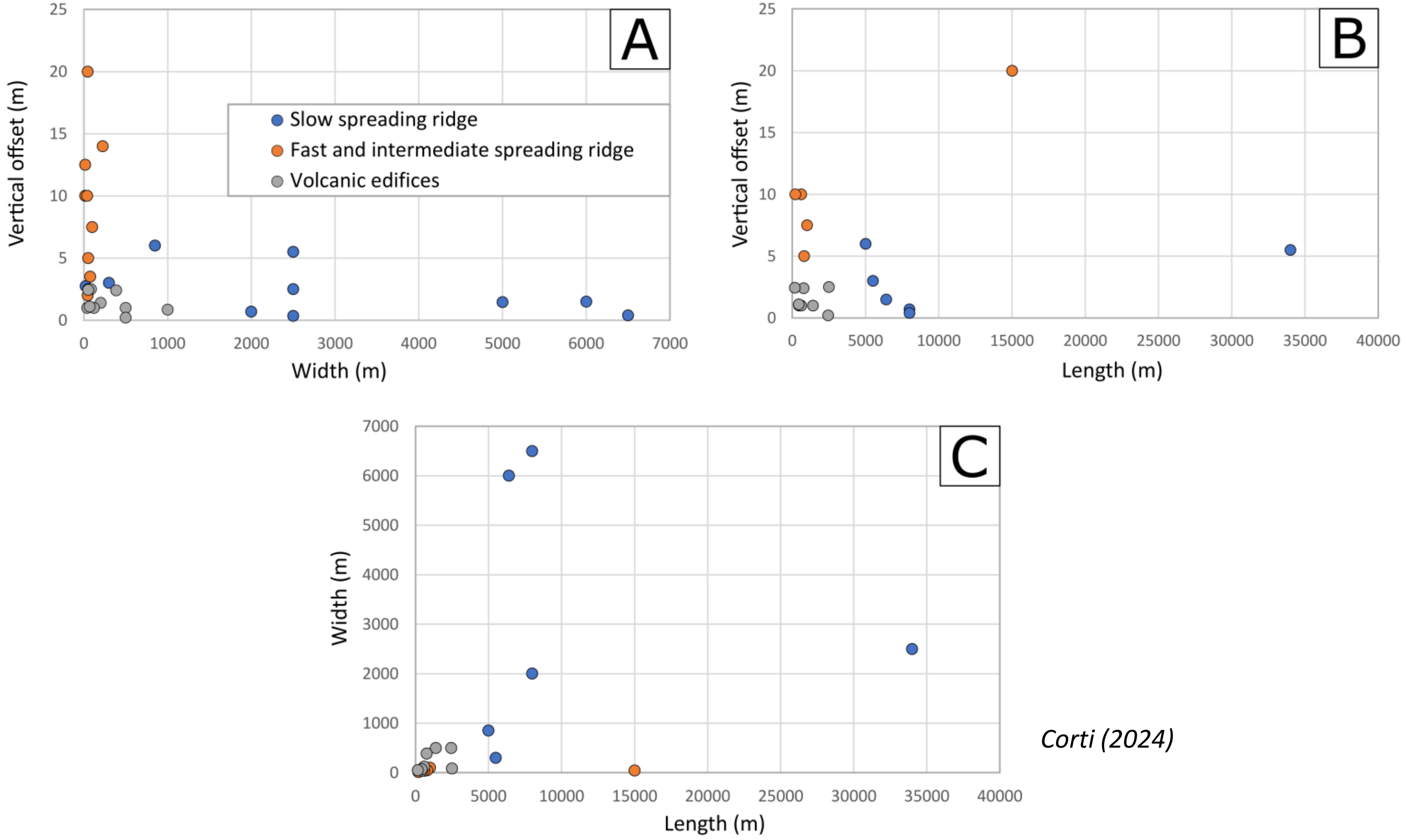

Corti (2024)

Discussion

What affects the geometry of dike-induced graben faults?

- **Dike inclination:** an inclined dike causes an asymmetrical distribution of stresses, that can explain **half-graben formation**.

- **Layering:** stiffness of the layers affects the **width of the graben at the surface**; soft layers distribute shear stress closer to the surface, favoring the formation of narrow grabens, whereas stiff layers tend to disperse shear stress, generating wider grabens.

- **Topography**: an inclined topography causes a rotation of the principal stresses, favoring **asymmetry of the graben faults**. Furthermore, the presence of high topographic scarps **affects the dike propagation path**, as highlighted by structural data on Mt. Etna.

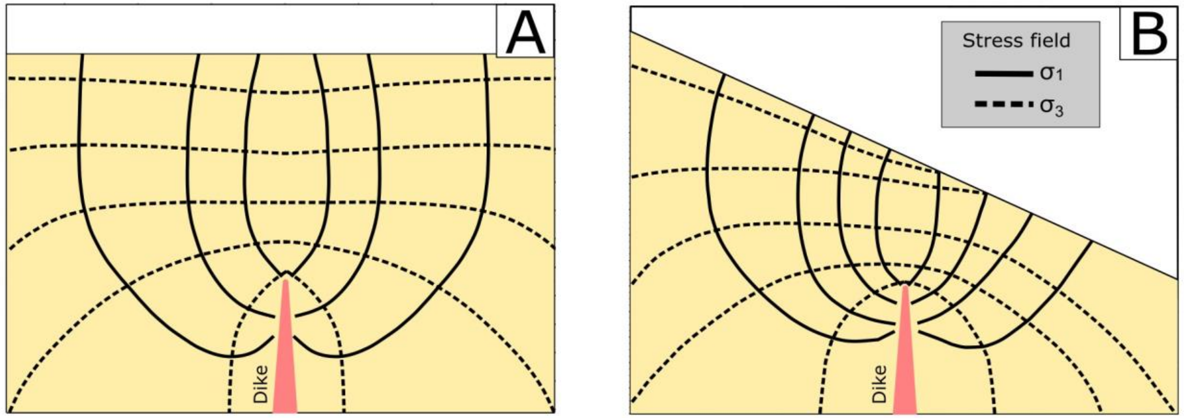

Corti (2024)

Discussion

Which parameters can favor the arrest of the dike?

If tensile stress at the dike tip becomes too low, the dike cannot propagate. Therefore, **the parameters that cause a decrease of tensile stress at the tip also favor the arrest of the dike**.

Furthermore, a dike can arrest its vertical propagation due to the presence of a **stress barrier, given by a 90° rotation of σ_1 and σ_3.**

- **Layering**: the 1928 fissure case suggested that **stiffness contrasts can create stress barriers.**
- **Compressional stress field**: the Stampar case shows that also a compression equal to or greater than dike overpressure can cause stress barriers.

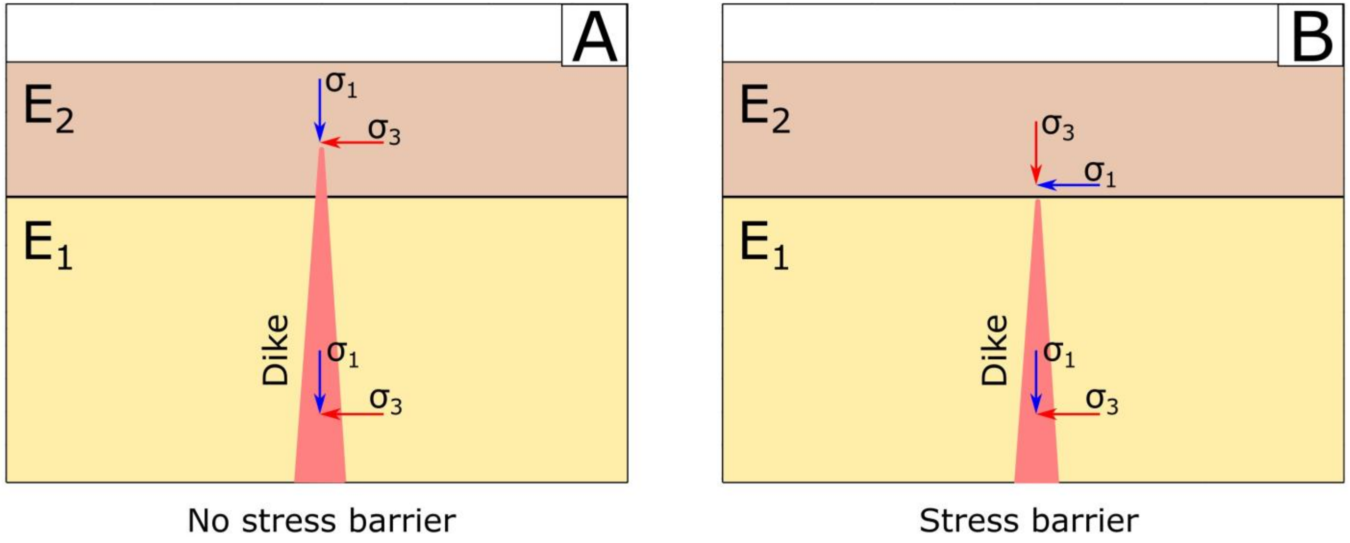

Corti (2024)

Conclusions

- This work analyzes the relation between **dike emplacement at shallow depth** and **brittle deformation at the surface**, as well as the factors that encourage **dike arrest during its vertical propagation**. The case studies are located at Mt. Etna (Italy) and in SW Iceland.

- **New structural data** were collected and were successively used as inputs for FEM **numerical modeling**, anchoring the models to field cases and making them realistic.

- Numerical models point out the **role of layering on dike-induced stresses**, with stiffer materials that concentrate stresses and softer materials that suppress them. In addition, stiffness affects the distribution of shear stress within the host rock.

- **Dike overpressure and inclination** affect its propagation and the concentration and distribution of dike-induced stresses.

- **Topographic variations** affect the dike propagation path and favor the asymmetry of the graben faults.

- Finally, **lateral compression** encourages dike arrest and the lack of brittle deformation at the surface. Numerical models therefore validate what was suggested by previous authors, only through conceptual models, regarding the geometry of dike-induced grabens along fast spreading plate boundaries.

References

Bonali, F.L., Corti, N., Pasquaré Mariotto, F., De Beni, E., Bressan, S., Cantarero, M., Russo, E., Neri, M., & Tibaldi, A. (submitted). 3D study of dyke-induced asymmetric graben: the 1971 Mt. Etna (Italy) case by structural data and numerical modelling. Journal of Structural Geology.

Corti, N. (2024). Analysis of deformation and stress regimes associated with dike emplacement. Doctoral dissertation, University of Milan-Bicocca.

Corti, N., Bonali, F. L., Russo, E., Drymoni, K., Mariotto, F. P., Gudmundsson, A., Esposito, R., Cavallo, A., & Tibaldi, A. (2023). Feeders vs arrested dikes: A case study from the Younger Stampar eruption in Iceland. Journal of Volcanology and Geothermal Research, 107914.

Drymoni, K., Browning, J., & Gudmundsson, A. (2020). Dyke-arrest scenarios in extensional regimes: Insights from field observations and numerical models, Santorini, Greece. Journal of Volcanology and Geothermal Research, 396, 106854.

Gudmundsson, A. (2011). Rock fractures in geological processes. Cambridge University Press.

Gudmundsson, A. (2020). Volcanotectonics: Understanding the structure, deformation and dynamics of volcanoes. Cambridge University Press.

Okada, Y. (1985). Surface deformation due to shear and tensile faults in a half-space. Bulletin of the seismological society of America, 75(4), 1135-1154.

Pollard, D.D., Delaney, P.T., Duffield, W.A., Endo, E.T., & Okamura, A.T. (1983). Surface deformation in volcanic rift zones. In Developments in Geotectonics (Vol. 19, pp. 541-584). Elsevier.

Saemundsson, K.; Sigurgeirsson, M.Á., Hjartarson, A.; Kaldal, I.; Kristinsson, S.G. (2016) Geological Map of Southwest Iceland, 1:100 000 (2nd ed.). Reykjavík: Iceland GeoSurvey.

Sæmundsson, K., Sigurgeirsson, M.Á., & Friðleifsson, G.Ó. (2020). Geology and structure of the Reykjanes volcanic system, Iceland. Journal of Volcanology and Geothermal Research, 391, 106501.

Tibaldi, A. (2015). Structure of volcano plumbing systems: A review of multi-parametric effects. Journal of Volcanology and Geothermal Research, 298, 85-135.

Tibaldi, A., Bonali, F.L., Russo, E., & Fallati, L. (2020). Surface deformation and strike-slip faulting controlled by dyking and host rock lithology: A compendium from the Krafla Rift, Iceland. Journal of Volcanology and Geothermal Research, 395, 106835.

Tibaldi, A., Bonali, F.L., Corti, N., Russo, E., Drymoni, K., De Beni, E., ... & Mariotto, F.P. (2022). Surface deformation during the 1928 fissure eruption of Mt. Etna (Italy): Insights from field data and FEM numerical modelling. Tectonophysics, 837, 229468.

Trippanera, D., Ruch, J., Acocella, V., & Rivalta, E. (2015). Experiments of dike-induced deformation: Insights on the long-term evolution of divergent plate boundaries. Journal of Geophysical Research: Solid Earth, 120(10), 6913-6942.